# Morphological instabilities and the dynamics of carbon nanotube forest growth

Finnie, P.; Vinen, P.; Marshall, P.; Lefebvre, J.



**Publisher's version / Version de l'éditeur:**
https://doi.org/10.1149/1.3655505
*ECS Transactions, 35, 25, pp. 3-12, 2011-05-01*

ECS Transactions, 35 (25) 3-12 (2011)
10.1149/1.3655505 ©The Electrochemical Society

# Morphological Instabilities and the Dynamics of Carbon Nanotube Forest Growth

P. Finnie[a,b], P. Vinten[b,a], P. Marshall[a], and J. Lefebvre[a]

[a] Institute for Microstructural Sciences, National Research Council Canada, Building M-50, 1200 Montreal Road, Ottawa, Ontario, K1A 0R6, Canada
[b] Department of Physics, University of Ottawa, 150 Louis Pasteur, Ottawa, Ontario, K1N 6N5, Canada

Vertically aligned carbon nanotube forests show various morphologies on both macro- and micro-scales. These morphologies are a result of growth mechanisms and interactions between nanotubes. By investigating these morphologies, we study both the growth mechanisms and the interactions. We examine forest morphologies *in situ*, dynamically during chemical vapor deposition growth and *ex situ*, post growth. *In situ* observations allow the separate characterization of nucleation, growth and termination phases, and the exploration of connections between morphology and growth. Forests systematically show different morphologies, ranging from uniform to cracked, delaminated, and periodically rippled. These are discussed in terms of the balance of forces within the forests including cohesion, adhesion, and stiffness. We propose a simplified model that predicts termination as a result of an imbalance in the forces present. We show that growth rate differences drive many morphological effects, and these differences originate in the nucleation phase due to gas diffusion.

## Introduction

One of the most successful approaches for the synthesis of carbon nanotubes has been chemical vapor deposition (CVD) using a carbon containing source gas and a substrate upon which a thin film or nanoparticle catalyst has been deposited (1,2). If the yield is high, growth can result in forests of nanotubes growing up out of the substrate. In recent years, vertically aligned carbon nanotube forests have been grown to increasing heights (3-6). For practical and purely scientific reasons, effects limiting the height are a subject of great interest. At the same time, there is immense variety in forests: they may consist of multiwalled carbon nanotubes (MWNT) or significant fractions of single walled nanotubes (SWNT), they can range in density, and they can show a variety of macro- and micro-scale morphologies which can change with time and film thickness. It is becoming apparent that additional effects govern the growth of ensembles of nanotubes beyond those governing individual nanotubes.

*In situ* studies are helpful to help clarify issues in the synthesis process, and vertically aligned carbon nanotube forests are especially suited to such studies (7), which can be as simple as observing the forest as it grows with a camera (8-12), for example in a cold wall CVD reactor. The earliest data from MWNT forests typically showed a constant rate

that would ultimately terminate, however at that time forest heights were limited, and the data was not well resolved. Since then, forest heights have been extended into the multi-millimeter and even centimeter regime, and the shape of the growth curves have been modeled and measured with higher fidelity.

In most cases, forests do not show a linear growth curve (constant growth rate). Usually, they tend to show an exponential deceleration in the height as a function of time (7,13). Ideally, nanotubes would grow indefinitely, to arbitrary lengths, but this exponential deceleration puts limits on the ultimate height for many processes. More recently it has become clear that forest heights often stop increasing abruptly (8,14-16). In a recent report nanotubes were grown to centimeter lengths without any apparent termination, though gradual termination was evident (6). Thus, for most synthesis processes the forest height is limited by either gradual or sudden termination. Gradual termination appears to have a plausible explanation in catalyst poisoning. There has been recent progress in understanding sudden termination, and several models have been proposed (15,17,18). One picture is that sudden termination comes simply from the cumulative effect of gradual termination, and the forest terminates once it falls below a threshold to be self-supporting (17). Another picture is that cross-linking of the top of the forest causes a force feedback which increases the free energy required to add carbon (18). We have proposed that strain building up in the layer may cause it to become favorable to delaminate or otherwise significantly alter the relationship between the catalyst and the substrate (15).

Distinct from termination, but likely related, is the morphology of the forest. Recently, investigating growth on finite sub-mm diameter catalyst islands we found that a variety of forest morphologies were routinely obtained (15). At low temperatures, much of the morphological evolution took place late in the growth, at least raising the possibility that it is connected with termination. We suppose that these morphological changes could be explained in terms of the driving force of growth rate differences and the physical/chemical nature of interactions between nanotubes and the substrate, nanotubes and themselves, and the inherent strength of nanotubes. Here we summarize some of these morphological changes, and discuss their origins and their magnitudes.

In this paper we show how non-uniform growth rates originate at the very earliest, nucleation stages of growth. We provide additional evidence to the growing body of data showing that the internal structure of a forest changes with time. We review several of the forces that must be considered when evaluating the interactions between nanotubes within a forest and explicitly explain how these forces could give rise to transitions in the (meta-)stable configuration of the forest morphology. It is predicted that the energetically favored state of the forest morphology depends on the lengths of the nanotubes present in the forest. We show that it is possible for a length dependent termination to originate from such a transition.

We have seen that morphology of these micro-patterned carbon nanotube forests is diverse, and at the same time the termination dynamics are surprisingly complicated. We consider the origins of these effects, and consider whether, and how, they may be related.

## Experimental

Carbon nanotube forests were grown by chemical vapor deposition using acetylene as the carbon source. The reactor is cold-walled with a resistive heater, and was operated at atmospheric pressure. The seed catalyst material was e-beam evaporated cobalt (0.8 nm) and alumina (250 nm) deposited on thermally oxidized silicon wafers which were patterned by shadow masking (100 μm to 800 μm diameter circles). The gas ratios during growth were acetylene (0.1%), with the assistance of water vapor (~0.1%), and hydrogen (0.5%), balance argon, supplied by a nozzle at an angle and arriving at a total flow of 0.25 L/min. The growth was tracked *in situ* with a camera and long working distance microscope optics directed at the growth sample at a glancing angle of ~5° to the plane of the sample (see figure 1). See our previous reports for a more detailed account (15).

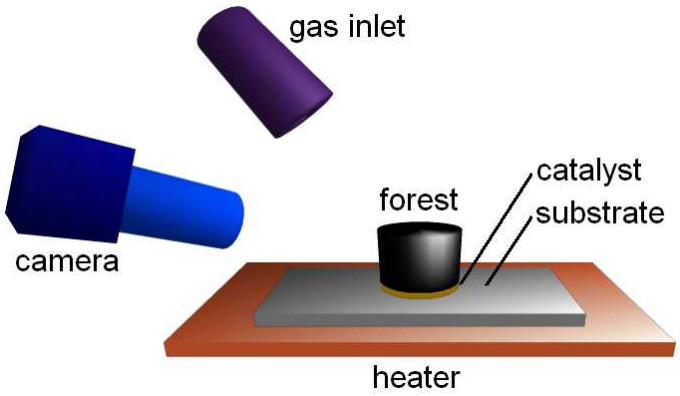


Figure 1. (Color online) Chemical vapor deposition reactor arrangement. Forests are grown by chemical vapor deposition and tracked optically *in situ* with a camera. A resistive heater is used. A thin film cobalt catalyst on alumina is prepared in circular islands on thermally oxidized silicon wafers. Source gases are supplied through a nozzle directed toward the substrate.

## Results

Previously, with this setup we observed the growth dynamics and extracted kinetic growth parameters for nanotube forests and how they changes with temperature. Briefly, over a large range in temperatures (~700°C - 900°C) the growth rate in terms of height vs. time shows an initial growth rate of about 1 μm/s, slowing very gradually with an exponential deceleration, until a critical point where the growth halts abruptly. The initial growth rate was found to decrease very slightly with increasing temperatures, with an associated (de-)activation energy of 200 meV. The magnitude of this energy suggests that hydrocarbon desorption from the surface is a possible explanation. Parasitic gas phase reactions which limit the supply of the active precursor could be another explanation for the gradual decrease with temperature.

The exponential decay can be extrapolated to a projected final height. This projected final height decreases rapidly with temperature, with centimeter scale projected heights for 700°C, and 100 μm scale heights at 900°C. The projected final height decreases with a (de-)activation energy of ~2 eV. The actual final height is much shorter at low

temperatures due to sudden termination, with millimeter scale heights realized for 700°C and 100 μm scale heights at 900°C with a projected cross-over between projected and actual final heights. The actual final height decreases with a (de-)activation energy of ~1 eV. The extremely different values of final height and projected final height, and their different scaling is a first hint that the mechanisms underlying the two could be different. In terms of the duration of growth, the projected lifetime ranges from hours at 700°C to minutes at 900°C, with an activation energy of ~2 eV, whereas the actual lifetime does not vary as much, is always on the order of 10 minutes, and shows no clear scaling with temperature. This is another way of looking at the data and also suggests a different mechanism for the two processes.

We also reported that the gross morphology of the forest islands varies. In figure 2 we take a new view at this type of data. Figure 2a shows the result of self-terminated growth at a relatively high temperature (860°C). A slightly concave top surface can be seen and the sidewalls curve inward somewhat. At lower temperatures, this concavity becomes more pronounced, as can be seen in figure 2b, which was terminated early by stopping the carbon supply. At lower temperatures, morphologies become even more complicated, with self-delamination common in the range 730°C and 760°C (figure 2c) and even cracking and "exploding" at lower temperatures (figure 2d). In the intermediate range of temperatures (~730°C to ~830°C), the forests reproducibly show periodic ripples on their outer surface of wavelength ~1 μm, extending over a large range (19,20). The ripples are so regular, over much of the forest height, that one can even obtain optical diffraction patterns from them.

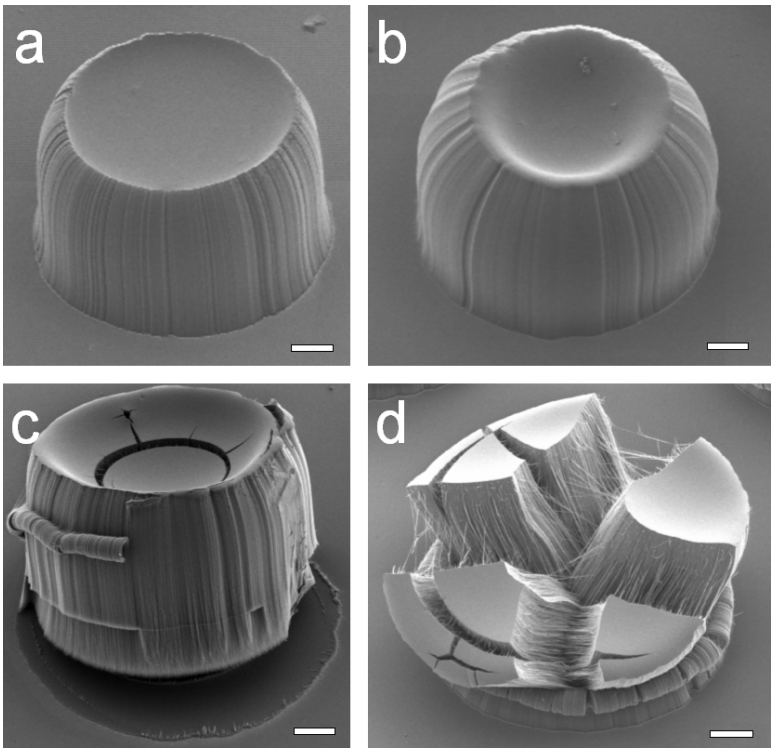


Figure 2. Morphologies of carbon nanotube forests. (a) Slightly concave, 860°C, self-terminated. (b) Pronounced concavity, 760°C, intentionally stopped. (c) Delaminated, 730°C, self-terminated. (d) Exploded, 720°C, self-terminated. All scale bars are 100 μm.

The concavity, rippling, and several other morphological changes are driven by variations in the growth rate across the catalyst island. *In situ* observations reveal that the growth rate difference is present at nucleation. Figure 3 shows a series of frames at 1 second intervals from a growth movie taken at 760°C on a 700 μm seed catalyst circle. Carbon growth on the catalyst island is black. It is clear that the growth is not uniform across the sample. Rather, in a cylindrically symmetric process, the growth is fastest at the outside, and fills in the interior later. The supply of reactive carbon is limited by diffusion of the gas to the growth sites. The outside part of the catalyst island receives extra supply due to the fact that carbon is not consumed by the surrounding exposed silicon oxide. The growth rate differences are driven by the supply of carbon, and by the consumption of carbon by other catalyst particles.

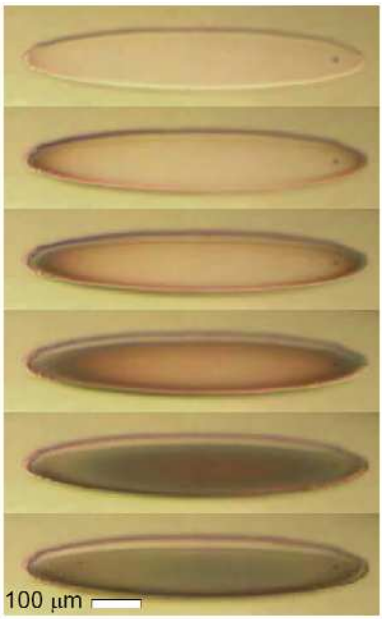


Figure 3. (Color online) Nucleation dynamics. A series of optical images from the camera looking into the reactor, taken at 1 second intervals, of a circular seed catalyst island at the onset of growth at 760°C.

In addition to the gross morphological changes of the forest, the internal arrangement of nanotubes, that is the internal morphology, is changed dramatically. Others have seen significant changes by other means. Nanotube diameters are reported to increase dramatically with forest height (21). Scanning electron microscopy and small angle X-ray scattering reveal that many forests become disordered before termination (14), and mass evolution experiments show that deceleration in the mass growth rate can precede sudden termination (17).

An interesting view of the evolution of the internal forest morphology is obtained simply by removing a forest island with sticky tape attached to the top. The forests stick more strongly to the tape than the substrate and are removed, intact, with virtually no

obvious change in overall shape after removal from the substrate. In figure 4a, the base of a forest in the steady growth phase at 760°C is shown as seen in a scanning electron microscope. In figure 4b an identically grown forest is shown immediately after sudden termination. It is clear that the base of the forest is much less dense at the termination stage, consistent with prior measurements.

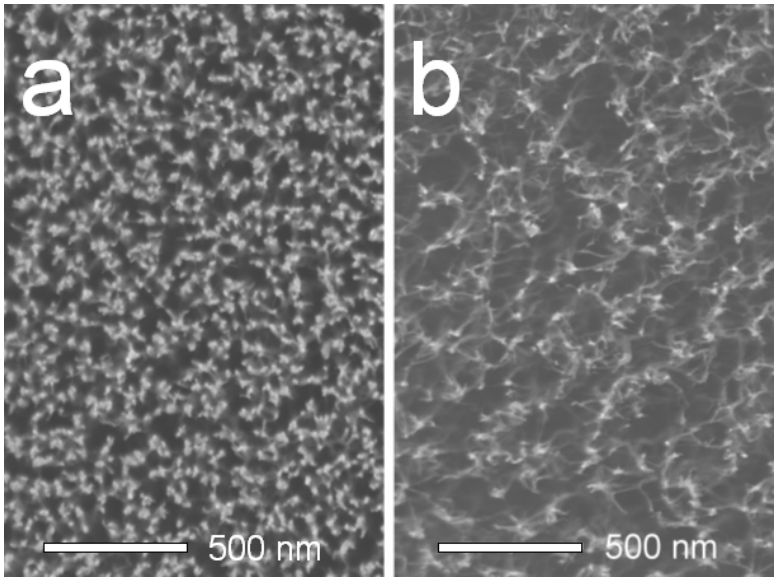


Figure 4. Root morphology. SEM images for an intentionally terminated forest (a) and for a self-terminated forest (b).

## Discussion

To try to understand the above morphological transitions, and the mechanisms of sudden termination, it is worth considering the physical/chemical interactions between nanotubes and their relative magnitudes. There are three obvious effects to consider, outlined in reference (15). Here we elaborate on that discussion. First there is the energy scale involved in keeping the nanotube in place. One can consider several effects. The seed particle should adhere to the substrate, the nanotube should adhere to the seed particle, and the nanotube must not break along its length. The lowest of all these energies is what limits the attachment of the nanotube to the substrate. The breakage of the nanotube along its length is then an upper limit to this energy. According to CRC tables, the energy to break a C-C bond is 6.4 eV (22). For a (25,0) SWNT as illustrated in figure 5a, it takes 160 eV at most to break the nanotube. This is an upper bound to the adherence/internal coherence of a SWNT.

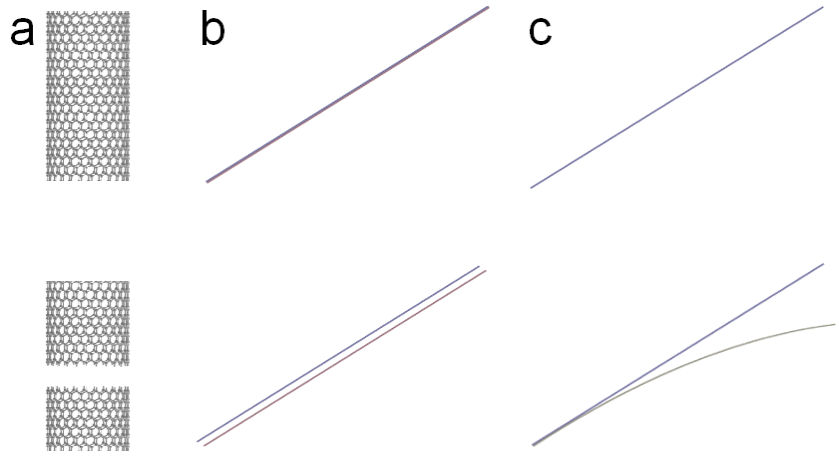


Figure 5. (Color online) Transformations requiring similar energies. (a) Breaking of the nanotube, or its adhesion to the substrate. (b) Debundling of a pair of nanotubes. (c) Deforming a nanotube.

Another interaction is the van der Waals interaction between the neighboring nanotubes. Graphene sheets adhere with an energy of ~20 meV/Carbon atom (23). A rigorous value for this cohesion energy is complicated by the fact that carbon atoms may or may not be registry, and the contact area between nanotubes depends on their diameters. If we consider (25,0) nanotubes, which are 2 nm in diameter, and suppose that they are effectively in contact with each other over a 1 nm width, we find that a 430 nm length is sufficient to build up a cohesion energy of 160 eV if we use the graphene surface density of 0.054 $nm^2$/C. Figure 5b is drawn to scale, showing the same amount of energy to debundle the pair as to break a nanotube.

Finally there is the mechanical stiffness of the nanotube. At a crude level of approximation this can be estimated from a rigid rod according to $E = \pi Y r^4 L / 8 R^2$, where, Y is Young's modulus (~1 TPa for a SWNT), r is the nanotube radius, R is the radius of curvature, and L is the length over which the nanotube is curved. If we consider the same 430 nm length (25,0) nanotube, 160 eV corresponds to a bend of radius of curvature of 2.5 μm. This is illustrated to scale in figure 5c.

These interactions can be used to explain the different morphologies, and the various morphological transitions. For these finite sized islands at the pressures used here, gas diffusion and catalyst activity give rise to the driving force of a non-uniform growth rate. The rippling instability can be understood by the buckling of the nanotube in response to the non-uniform growth rate. The wavelength of rippling can be roughly predicted if it is determined by the need to balance cohesion and bending (20). A 0.1 μm scale bending radius is predicted if the cohesion energy and bending energies are equivalent, with the great uncertainty regarding choice of contact area. Nonetheless, this very crude approximation predicts the observed rippling scale.

The cracking and exploding morphology is understandable if the strain energy can be reduced by debundling nanotubes. The delaminated morphology can be understood if strain energy can be reduced by severing the nanotube from the substrate. At low temperatures, both these processes often occur in late phases of the growth of finite

forests. It is worth pointing out that a forest of nanotubes is only ever in some metastable state. The minimum energy configuration would be graphite under ordinary conditions. It is also worth pointing out that in order to make a transformation between states, an activation energy would ordinarily be involved and so there is a kinetic element to making the transition. That is, even though the transition may be energetically favored, it must also be reached in a short enough time scale.

Finally we explicitly consider two simplified scenarios in which transitions between growth modes may be expected as nanotube lengths increase. These are scenarios which could terminate nanotube growth. Whether or not they are responsible for sudden termination, such transitions should be possible to observe under the right conditions.

The first scenario is likely not the origin of the transition, however, it illustrates very clearly how such a transition could take place by balancing two effects. It involves the balance of adhesion with cohesion and is illustrated schematically in figure 6. Considering two nanotubes, one possible configuration is for both nanotubes to adhere to their catalyst particles, and to be otherwise separate (figure 6a). The adherence to the catalyst particle saves some energy, but there is no energy saving from bundling. This configuration is more favorable for short nanotubes. Another possible configuration is for the nanotubes to bundle together, which decreases the total energy, but to do so, they may need to detach from the catalyst (figure 6b). This is more energetically favorable for longer nanotubes. Formally if an energy A is saved by attachment, and an energy B per unit length L is saved by bundling, then the total energy is $E = -2A$ for the initial configuration, and $E = -A - BL$ for the final configuration. There is then a cross-over length of $L = A / B$. This length holds for a generalization to many nanotubes. As an example, if *A* is 160 eV and B is 20 meV/nm, the transition occurs after 8 μm of contact length. If nanotubes are in contact over a smaller area, as would be the case for meandering nanotubes, this transition would occur at a proportionally larger length.

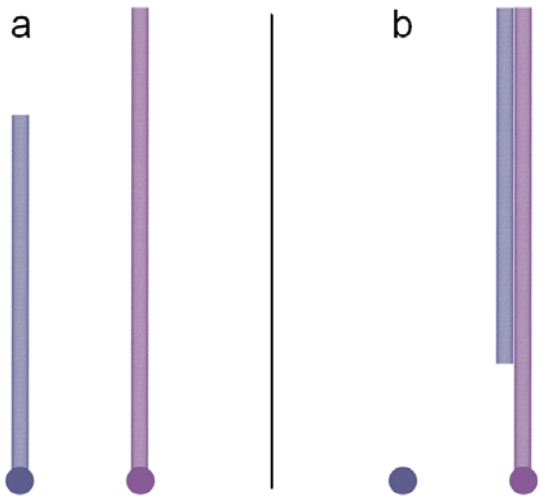


Figure 6. (Color online) Balancing adhesion with cohesion. (a) Nanotubes adhering to catalyst particle. (b) One nanotube detached and bundled.

The second scenario is more realistic, would appear to explain morphological changes, and may help explain sudden termination. However, it is harder to parameterize mathematically because it is more dependent on the precise geometrical configuration of the forest. Consider two nanotubes growing from two seed particles which are bound together at the top by van der Waals forces (figure 7). If the nanotubes grow at different rates, strain can build up as the nanotubes lengthen and try to satisfy the constraints of cohesion between nanotubes and adhesion to the catalyst particle (figure 7a). Strain energies can be relieved by breaking the adhesion to the nanoparticle (figure 7b). The latter scenario becomes more favorable as more strain builds up. This may explain delaminated morphologies and is also a potential explanation for sudden termination. Another way to relieve the strain is to maintain the adhesion to the substrate, but to break the van der Waals cohesion, and this would explain the cracking morphology.

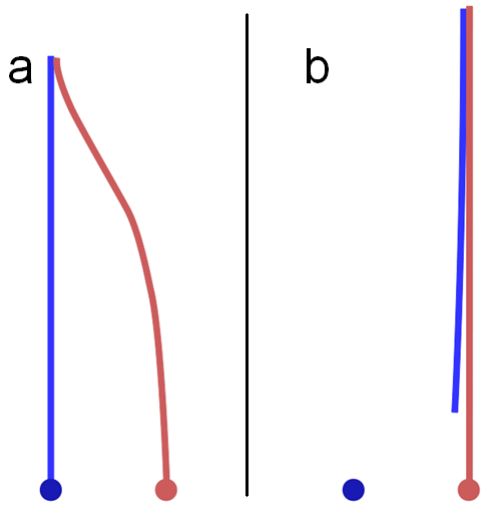


Figure 7. (Color online) Balancing adhesion with strain. (a) Both nanotubes adhering to seed particles, with one strained. (b) One nanotube detached and strain relieved.

## Conclusions

*In situ* observations show that gradual and sudden termination show different scaling. On sub-millimeter scale catalyst patterns, drastic gross morphological changes occur which may also be related to termination. The morphological changes are driven by non-uniform nanotube growth rates, which begin in the nucleation stage. At the same time, the microscopic morphology of the forest at the base is very different for a self-terminated forest as compared to an intentionally terminated forest. Forest morphologies can be interpreted in terms of the effects of adhesion, cohesion, and strain. Simplified models balancing adhesion with cohesion or adhesion with strain predict a cross-over from adherence to detachment. Thus, morphology and termination might be connected in such a fashion. Regardless, to understand forests it has become necessary to move beyond considering them as simply collections of non-interacting nanotubes growing independently. Collective effects must be considered.

## Acknowledgments

We are grateful to Hue Tran, Mike Denhoff, and Jeff Fraser for technical assistance at various stages of this work. We are grateful for funding from an NSERC Discovery Grant, an NSERC CGS, and an NRC GSSSP.

## References

1. Z. F. Ren, Z. P. Huang, J. W. Xu, J. H. Wang, P. Bush, M. P. Siegal, and P. N. Provencio, *Science*, 282, 1105 (1998).
2. J. Kong, H. T. Soh, A. M. Cassell, C. F. Quate, and H. Dai, *Nature*, 395, 878 (1998).
3. Y. Murakami, S. Chiashi, Y. Miyauchi, M. Hu, M. Ogura, T. Okubo, and S. Maruyama, *Chem. Phys. Lett.*, 385, 298 (2004).
4. K. Hata, D. N. Futaba, K. Mizuno, T. Namai, M. Yumura, and S. Iijima, *Science*, 306, 1362 (2004).
5. G. Zhong, T. Iwasaki, J. Robertson, and H. Kawarada. *J. Phys. Chem. B*, 111, 1907 (2007).
6. S. Yasuda, D. N. Futaba, T. Yamada, J. Satou, A. Shibuya, H. Takai, K. Arakawa, M. Yumura, and K. Hata, *ACS Nano*, 3, 4164 (2009).
7. A. A. Puretzky, D. B. Geohegan, S. Jesse, I. N. Ivanov, and G. Eres, *Appl. Phys. A*, 81, 223 (2005).
8. A. A. Puretzky, G. Eres, C. M. Rouleau, I. N. Ivanov, and D. B. Geohegan, *Nanotechnology*, 19, 055605 (2008).
9. I. Gunjishima, T. Inoue, and A. Okamoto, *Appl. Phys. Lett.*, 91, 193102 (2007).
10. A. J. Hart, L. van Laake, and A. H. Slocum, *Small*, 3, 772 (2007).
11. S. Yasuda, D. N. Futaba, M. Yumura, S. Iijima, and K. Hata, *Appl. Phys. Lett.*, 93, 143115 (2008).
12. P. Vinten, J. Lefebvre, and P. Finnie, *Chem. Phys. Lett.*, 469, 293 (2009).
13. D. N. Futaba, K. Hata, T. Yamada, K. Mizuno, M. Yumura, and S. Iijima, *Phys. Rev. Lett.*, 95, 056104 (2005).
14. E. R. Meshot and A. J. Hart, *Appl. Phys. Lett.*, 92, 113107 (2008).
15. P. Vinten, P. Marshall, J. Lefebvre, and P. Finnie, *Nanotechnology*, 21, 035603 (2010).
16. S. Noda and H. Sugime, *Carbon*, 48, 2203 (2010).
17. M. Bedewy, E. R. Meshot, H. Guo, E. A. Verploegen, W. Lu, and A. J. Hart, *J. Phys. Chem. C*, 113, 20576 (2009).
18. J.-H. Han, R. A. Graff, B. Welch, C. P. Marsh, R. Franks, and M. S. Strano, *ACS Nano*, 2, 53 (2008).
19. P. Vinten, J. Lefebvre, and P. Finnie, *Appl. Phys. Lett.*, 97, 101901 (2010).
20. P. Vinten, J. Bond, P. Marshall, J. Lefebvre, and P. Finnie, *Carbon*, in press (2011).
21. K. Hasegawa and S. Noda, *Appl. Phys. Express*, 3, 045103 (2010).
22. Y.-R. Luo, *Bond Dissociation Energies* in *CRC Handbook of Chemistry and Physics, 89th Edition*, D. R. Lide, Editor, CRC Press/Taylor and Francis, USA (2009).
23. M. C. Schabel and J. L. Martins, Phys. Rev. B, 46, 7185 (1992).